International Journal Of
Industrial Electronics Control and Optimization
Print ISSN: 3517-2645
Online ISSN: 3568-2645
Homepage: https://ieco.usb.ac.ir/

Comparative Study of AI Models for Multi-Level Optimization of External Lightning Protection Systems in Photovoltaic Stations

Hamid Reza Sezavar
Department of Electrical and Computer Engineering, Qom University of Technology, Qom, Iran.
Corresponding author's email: sezavar@qut.ac.ir

Article Info

Article type:
Research Article
Article history:
Received: **********
Received in revised form: **********
Accepted: **********
Published online: **********
Keywords:
ELPS,
Grounding electrode,
Lightning protection,
PV station,
Multi-stage AI.

ABSTRACT

This paper presents a comparative study on the application of artificial intelligence (AI) for optimizing External Lightning Protection Systems (ELPS) in photovoltaic power (PV) plants. The research addresses the critical need for advanced protection systems in solar installations, which are particularly vulnerable to lightning strikes due to their expansive outdoor configurations. Through a detailed comparative analysis, the study evaluates multiple AI approaches, including metaheuristic algorithms and machine learning models. The investigation reveals that metaheuristic algorithms often have lower accuracy compared to modern AI techniques. All comparisons are based on a multi-level optimization framework, systematically addressing air termination design, grounding system configuration, and overall system integration. The results show superiority in sensitivity analysis in the transformer model. Compared to other models, the random forest (RF) model, along with the artificial neural network (ANN) model, has a higher speed in data analysis. However, physics-informed neural networks (PINN) achieve remarkable improvements, delivering 93% protection coverage with only 3.2% grounding error while significantly reducing design convergence times.

NOMENCLATURE

A_p	Protection area provided by termination rods	r	Radius of the rolling sphere
A_{pv}	Total area of the PV power plant	r_p	Protection radius of an air termination pole
d_e	Diameter of a ground electrode	R_e	Resistance of a single ground electrode
D	Distance between the electrodes	R_{e_0}	Ground resistance while the soil moisture is zero
h_p	Height of an air termination pole	R_t	Total resistance of the entire grounding system
I_{max}	Maximum lightning current	T_d	Number of thunderstorm days per year
k	Grounding electrode spacing factor	V_{max}	Maximum lightning voltage
L_e	Length of a ground electrode	α	Protection angle
N_e	Number of ground electrodes	ρ	Soil resistivity
N_p	Number of air termination poles	ψ	Protection Level
m	Moisture percentage	σ	Empirical constant depending on the soil conditions

I. Introduction

A. Motivation

Lightning occurs when the imbalance in electrical charges between clouds or between clouds and the ground becomes too great, leading to a sudden discharge [1, 2]. The basic principle of lightning protection is to create controlled paths that can safely conduct the resulting high current to the ground. While arresters effectively control lightning currents in power systems [3], installations at risk require additional protection. This is why comprehensive external lightning protection systems (ELPS) are implemented. These types of protection systems can provide complete protection in addition to arresters [4, 5]. An adequately designed ELPS consists of three critical components that work together. Aerial terminals prevent lightning strikes, down conductors conduct the current downward, and an extensive grounding system safely dissipates the energy to the ground [6]. This rapid deflection serves two critical purposes: it prevents equipment damage from surges while significantly reducing the risk of damaging electromagnetic induction in adjacent

systems [7]. While these protection systems are essential for electrical infrastructure, they are equally critical for any structure vulnerable to lightning, including commercial buildings, industrial facilities, and especially solar power installations [8]. Solar farms present unique challenges in lightning protection due to their outdoor locations. Their vastness makes them prime targets for lightning. When lightning strikes an unprotected solar array, it affects all PV elements. PV panels can be destroyed, inverters can be damaged, and connection systems can melt. For these reasons, a thorough lightning risk assessment and properly engineered protection systems are not only recommended for solar installations but are critical for financial and operational sustainability [9].

B. Literature review

Recent advances in ELPS modeling have shifted from traditional approaches to advanced AI-based techniques. Much research has been conducted on computational methods for optimizing lightning protection systems. For example, in [10, 11] used genetic algorithms (GA) to model ground electrode configurations, while another study [12] used random forest classification [13] to analyze weather patterns for lightning prediction. Simulation-based approaches have also been valuable, and mathematical algorithms have been applied to design efficient grounding systems [14]. This field has seen interesting advances in optimization algorithms. Studies [15-19] have compared particle swarm optimization (PSO), genetic algorithms, and hybrid HGA-PSO methods for grounding system design. Recently, neural network approaches have emerged as promising alternatives. In [20] introduced a multi-stage neural network model that proposed innovative ELPS configurations – using fewer but taller poles and shorter ground electrodes compared to traditional ATP/EMTP methods. Beyond electrical performance, contemporary research has begun to examine practical installation factors.

The effects of protection poles' shading on solar panels have become an important design consideration. A case study [21] of an 8 MW solar power plant demonstrated a successful balance of concerns related to shading, tower height, and current discharge capacity. Comprehensive analyses [22] have also confirmed that passive ELPS isolated with galvanized grounding provides optimal protection for photovoltaic installations. Comparison of algorithms has yielded valuable insights. When the NSGA and MOPSO methods [23] were tested for distribution system protection, the results showed that NSGA exhibited superior performance in both grounding optimization and overall system reliability enhancement. Parallel research [24, 25] specifically focused on minimizing the impact of lightning rod shading while maintaining protection effectiveness—a critical consideration for solar farm layouts.

C. Contributions

According to the literature review, ELPS design studies have moved towards the use of artificial intelligence (AI) models. Where traditional methods rely on empirical calculations and manual iterations, modern research increasingly employs both meta-heuristic optimization techniques and machine learning models to solve this complex engineering challenge. While meta-heuristic methods have dominated early applications, machine learning approaches are now demonstrating remarkable potential when supplied with comprehensive training datasets that capture real-world variability. Perhaps less than machine learning models are used for optimization, but with appropriate training data, a suitable system can be designed to optimize and estimate ELPS parameters. Therefore, considering the gap in optimization studies based on artificial intelligence, this article has reviewed and compared artificial intelligence models that can be used for optimization in ELPS design. It is worth mentioning that multi-level optimization models are used to estimate parameters in a step-by-step manner. This comparative investigation evaluates artificial intelligence models across the full spectrum of design conditions encountered in practice. The analysis considers how different models respond to variations in local weather patterns, including thunderstorm frequency, site-specific photovoltaic array characteristics, soil conductivity properties, and international protection standards. As a result, the best model can be selected for design considering all conditions.

D. Paper organization

The rest of this paper is structured as follows: Section 2 details the External Lightning Protection System that would cover air termination parameters and grounding system design. Section 3 introduces the proposed multi-level optimization framework in ELPS. Section 4 presents the results and comparative analysis, and discussion. Finally, Section 5 summarizes the conclusions and discusses implications for future research.

II. External Lightning Protection System

ELPS provides power system protection at the desired level in an outdoor environment. ELPS consists of two parts: air terminal and ground connection. The parameters of the air terminal include the height of the poles (*hp*) and the number (*Np*). The coverage area is estimated based on the pole protection radius (*Rp*). In addition to these parameters, the parameters of the ground system include the number of electrodes (*Ne*), electrode length (*Le*), and electrode diameter (*de*). Electrical indices, including the resistance value of each electrode (*Re*) and the total resistance (*Rt*), are calculated using these parameters. Considering the importance of using ELPS in outdoor solar power plants, it is valuable to design the optimal parameters according to the constraints of a PV power plant.

A. Air Termination Parameters

The first component of an ELPS system that is usually struck by lightning is the aerial terminal. The installation height of this terminal (*hp*) plays a decisive role in the efficiency of the protection system, as it directly affects the size of the protection radius. Based on the accepted principle that lightning strikes the highest point in an area, as the installation height increases, the radius of the area covered by the protection increases, while the corresponding protection angle decreases. This relationship is shown in Equation (1)[7]:

$$r_p = h_p \times tan\alpha \quad (1)$$

In this regard, α represents the protection angle. As can be seen, although increasing the height increases the area covered by the protection, it also decreases the protection angle. For this reason, instead of increasing the height, a more efficient option is to increase the number of protection rods. Proper distribution and dispersion of the protection rods provides a better solution than increasing the height. Other factors also play a vital role in the design of this system, including the required protection level and the frequency of lightning days in the area. The average number of days with lightning in an area can be an effective indicator for determining the optimal number of protection rods required to achieve the desired protection level. An increase in this average means an increase in the probability of sudden lightning strikes, and as a result, increases the necessity of deploying the ELPS system in various areas. To calculate the radius of protection (*rp*) and measure the area covered, the standard "rolling sphere" method is used. The geometric performance of this method is illustrated in Figure 1. In accordance with the IEC standard and using the radius of the rolling sphere (*r*) whose values are given in Table I, the value of *rp* can be obtained through the following equation: [26, 27]:

$$r_p = \sqrt{h_p(2r - h_p)} \quad (2)$$

therefore, the protection area (A_p) can be calculated as follows:

$$A_p = \pi {r_p}^2 \quad (3)$$

B. Grounding Parameters

The grounding system, as a vital component of the ELPS, plays a crucial role in transferring the fault current to the ground. The resistance value of the grounding electrode depends on factors such as the length of the rod and the distance between the electrodes. This resistance can be calculated using the following equation [28]:

$$R_e = \frac{\rho}{2\pi L_e}\left(Ln\left(\frac{4L_e}{d_e}\right) - 1\right) \quad (4)$$

where ρ is the specific resistance of the soil. Considering the importance of the number of electrodes, the total resistance is calculated with the number of electrodes as follows [29]:

$$R_t = \frac{R_e}{N_e}\left(1 + \frac{N_e - 1}{2}k\right) \quad (5)$$

where k is the space factor and can be calculated according to the following equation [28-30]:

$$k = \frac{1}{\ln\left(\frac{D}{d_e}\right)} \quad (6)$$

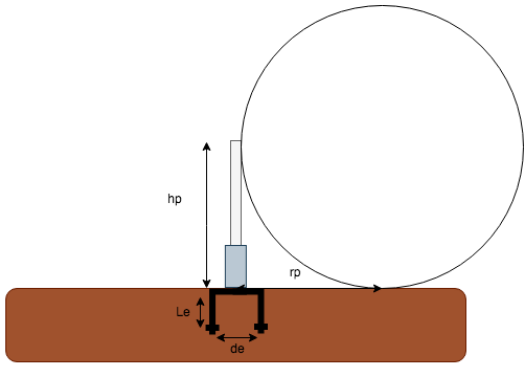

Fig. 1. Schematic view of rolling sphere method geometry.

TABLE I. IEC standard lightning protection level classification.

Protection levels	radius of rolling sphere (m)	Description
1	20	Highly critical structures
2	30	Important infrastructure
3	45	Standard commercial structures
4	60	Low-risk structures

where D is the distance between the electrodes. The parameters of the number of electrodes, their length, diameter, and distance between them play a significant role in eliminating the fault caused by lightning. The specific resistance of the soil based on [31] can have different values according to the humidity and climate of the region. However, from an electrical perspective, the maximum current during a fault should be reasonably correlated with the resistance value of the electrodes. Optimal resistance values ensure the effective conduction of electrical current in the soil environment, allowing for safe fault clearance. According to [32], the maximum current that the ELPS is able to protect, can be approximated through the following:

$$I_{max} = \sqrt[0.75]{r} \quad (7)$$

Based on the protection level, the value I_{max} is calculated. According to [33], based on the maximum lightning voltage in an area, the grounding resistance relationship can be expanded as follows:

$$R_e = R_{e_0} e^{-\sigma m} \quad (8)$$

where R_{e_0} is earth resistance while the soil moisture is zero, m is the moisture percentage, and σ is an empirical constant depending on the soil conditions. In order to simplify the calculation of the electrode resistance, the following equation can be proposed to estimate it based on electrical parameters:

$$R_e = \frac{V_{max}}{I_{max}} \times e^{-\sigma m} \quad (9)$$

Therefore, considering equations (7) and (9) and also the relationship with them, equations (4) and (5), the number of electrodes (N_e), their length (L_e), and their diameter (d_e) can be calculated based on the maximum protective current [32, 34, 35].

III. Multi-Level Optimization in the ELPS

According to the different parts of ELPS that are explained in the previous section, its design includes several interconnected parameters. In the first stage, the goal is to design the optimal air termination parameters. *Np* and *hp* are calculated according to the input data based on Equations (1) and (2). The input data include the PV area and PV parameters, the protected area, and the number of thunderstorm days. According to [20], there is a relationship between *Td* and the optimal number of *Np*. This relationship is obtained according to the training data of the first stage neural network by the artificial intelligence model and is considered in the optimal design. Finally, the defined input variables are considered to produce the *Np* and *hp* outputs, and the following equation is defined:

$$N_p, h_p = f_{AI1}(T_d, A_p, \Psi)$$
$$subject\ to: r_p = \begin{cases} hp \cdot \tan\alpha \rightarrow (Eq.1) \\ \sqrt{hp(2r-hp)} \rightarrow (Eq.2) \end{cases} \quad (10)$$

where Ψ denotes the protection level (IEC standard), and r is the rolling sphere radius from Table I. In Equation (10), the model *fAI1* predicts the optimal number of air termination poles (*Np*) and their heights (*hp*) using inputs such as thunderstorm days (*Td*), protected PV area (*Ap*), soil resistivity (ρ), and the protection level (Ψ). The protection radius (*rp*) is derived via either the empirical tangent method or the rolling sphere method (IEC 62305), ensuring compatibility with site-specific requirements. This replaces traditional heuristic approaches with a data-driven model trained on historical lightning strike data and PV plant configurations. The objective of the first optimization level is to determine the optimal configuration of the air termination system. The primary goal is to minimize both the number and height of protection poles. The design variables for this level are formally defined as the vector $X_1 = [Np, hp]$. This optimization is subject to several critical constraints. First, the total area of the photovoltaic plant (*Apv*) must be completely contained within the total protected area, governed by the inequality $Apv \sim \leq Np \times \pi \times rp^2$. Second, the protection radius for each pole must be derived strictly in accordance with the IEC 62305 standard, based on the selected protection level (Ψ) and its corresponding rolling sphere radius, as specified in Table I. The governing equation for the protection radius, Equation 2, ensures the design adheres to the standardized rolling sphere method. The outputs of the first stage are considered as the input of the second stage. Also, according to the calculation of *hp* and *Np* and Table I, the ground resistance can be calculated using Equations (7) to (9). This resistance can be measured based on the outputs of the first stage, including *hp* and *Np*, using Table I to calculate *Re* and finally using the maximum lightning voltage and current. In this study, the maximum lightning voltage is assumed to be constant. The following formula is also designed for optimization in the second stage to calculate *Re*:

$$Re = f_{AI2}(h_p, N_p, V_{max}, I_{max})$$
$$with: I_{max} = \sqrt[1/4]{r}\ (from\ Eq.7) \quad (11)$$

The second level focuses on defining the performance requirement for the grounding system. The key variable for this stage is $X_2 = [Re]$. It must be sufficiently low to ensure that the voltage rise during a maximum fault current does not exceed the system's insulation withstand capability. This fault current level (*Imax*) is naturally linked to the protection level. It is calculated via the governing Equation 7. The target resistance is therefore not a fixed value but a function of the outputs from first stage and the chosen protection level.

In the third stage, the output of the second stage is considered as an input. Considering the soil resistivity (ρ), the desired total resistance (*Rt*), and the electrode spacing coefficient (k), the number of electrodes (*Ne*) and the length of the electrodes (*Le*) can be calculated based on equations 4 to 6. In this case, the optimization equation of the third stage is defined as follows:

$$N_e, L_e, D = f_{AI3}(R_e, \rho, k),$$
$$constrained: R_t = \left(\frac{N_e}{R_e}\right)\left(1 + \frac{(N_e - 1)}{(2\ln(D/d_e))}\right) \quad (12)$$

In the third stage, according to the output of the second stage, equation 4 is formed. This is the first optimization constraint in this stage. Then, equation 5 is developed according to the total resistance requirement, and the second constraint is also established. This constraint, along with Equation 6, is actually the basic constraint of this stage. Therefore, using this constraint, the optimization model can be run, and the best values for RE and LE can be calculated.

Table II is a representation of some of the data used to train the neural network used in this study. The data in Table II is a hybrid dataset, combining simulated parameters in ATP/EMTP with relationships derived from the cited literature and standards. This data has been collected based

on [35, 36] studies. The machine learning optimization process is a multi-level approach that separates the design of all parameters into three sections. First, various AI models are trained on an extensive historical dataset that matches site conditions—like the number of local storm days, the size of the solar farm, and soil type—to their optimal protection system parameters. Once trained, this AI assistant is used in a practical, three-step design process. In the first step, it takes the new site's conditions and instantly predicts the best number and height for the lightning poles. The results from this step are then passed to a second AI model, which calculates exactly how low the electrical resistance of the grounding system must be to handle the energy from a strike safely. Finally, a third AI model uses that resistance target to design the physical grounding system itself, specifying the number, length, and diameter of the ground rods needed.

TABLE II. Neural network training dataset specifications

Td	*Apv*	*Ap*	*ρ*	*Rs*	*Rt*	*k*
130	5369	6563	30	7.32	1.85	0.13
102	20164	21737	300	46.79	12.70	0.18
109	17984	22269	150	18.52	5.51	0.13
124	10438	13769	400	88.70	48.02	0.17
127	31533	34281	1000	139.74	75.15	0.15
114	25262	25850	100	12.48	3.17	0.13
115	14500	18000	50	9.45	2.50	0.14
108	22000	24000	200	25.30	7.80	0.16
121	8500	12000	250	65.20	32.10	0.19
132	42000	45000	800	120.50	65.30	0.14
105	18000	21000	120	15.75	4.20	0.12
118	32000	35000	600	95.40	52.60	0.17
126	12500	16000	350	72.80	40.50	0.18
111	19500	23000	180	22.10	6.90	0.15
129	38000	41000	900	130.20	70.80	0.16
107	16500	19000	90	11.20	3.05	0.13

In general, what distinguishes multi-level optimization based on artificial intelligence from traditional models is the unique ability to find optimal points concerning suitable training data. If the data is selected appropriately, this type of optimization can bridge the gap between heuristic and meta-heuristic models such as genetic, PSO, and other such models. In this study, an attempt has been made to examine various artificial intelligence models for the purpose of multi-level optimization and to present a comprehensive comparative study. Each of these models has its strengths and weaknesses in the design of ELPS in a PV system. Finally, considering the different inputs, a suitable model can be designed for the design of an ELPS suitable for installation in a PV power plant.

Figure 2 shows the proposed scheme for optimizing the design of a lightning protection system. The model breaks down a significant, complex problem into three smaller, easier-to-understand parts. The first step is to design the lightning rods. The AI uses information about the weather, the size of the solar farm, and safety standards to decide on the number of rods needed and their height. This solves the problem of protecting the area from lightning strikes. The second step uses the results of the first step to calculate the target of the grounding system. This step determines how low the electrical resistance should be to handle lightning energy safely. This step connects the design of the above-ground rods to the underground electrodes. The final step is to design the grounding system itself. Using the resistance target from the second step, the AI calculates how many ground rods are needed, how long they should be, and how wide they should be. This ensures that the lightning current can be safely absorbed into the ground.

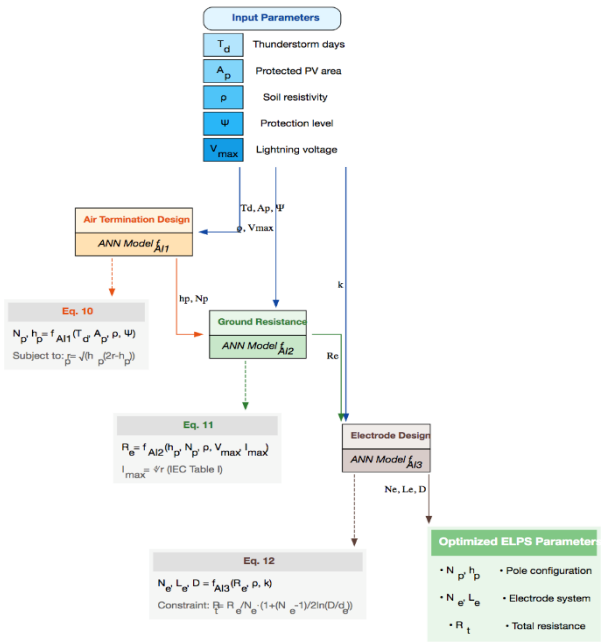

Fig. 2. Flowchart of multi-level optimization framework.

IV. Results and Discussion

In order to analyze the presented model, according to the flowchart of Figure 2, 400 test data samples based on Table II have been examined. The PINN, RF, Transformer [37, 38] , and artificial neural network (ANN) [39, 40] models have been implemented for AI purposes. The GA, PSO, and HGA-PSO models have been changed to metaheuristic models [41, 42].

A. Performance Analysis

Optimization of ELPS for PV power plants requires a careful examination of computational efficiency and protection effectiveness. A comparative analysis between traditional metaheuristic approaches and modern AI-based methods is investigated in three criteria: convergence time,

protection score, and ground fault. The results of these investigations are shown in Table III.

In the first part, the convergence time is investigated based on the same data. Genetic algorithms (GA) show the slowest approach with 142 seconds, while particle swarm optimization (PSO) shows a 31% improvement with 98 seconds. The combined HGA-PSO method has a more suitable improvement with convergence in 76 seconds due to the integration of the effective points of both previous algorithms. However, AI models show superior efficiency, with RF providing the fastest results in only 18 seconds. The ANN model shows an average result of 22 seconds. Physics-based neural networks require a slightly longer time of 28 seconds due to their inherent physical limitations, while transformers come in at 34 seconds. This significant time reduction – up to 88% compared to GA – allows for rapid design iterations and real-time adjustments as environmental conditions change.

TABLE III. Comparative performance metrics of optimization methods

Method	*Convergence Time*	*Protection Score*	*Grounding Error*
GA	142 sec	82%	12.3%
PSO	98 sec	85%	9.7%
HGA-PSO	76 sec	88%	7.1%
ANN	**22 sec***	91%	5.9%
PINN	28 sec	**93%**	**3.2%**
Transformer	34 sec	90%	4.1%
RF	**18 sec***	89%	6.7%

The *Protection Score* is a quantitative metric that evaluates the effectiveness of the air termination system design. It is calculated as the percentage of the total photovoltaic plant area (A_{pv}) that is successfully covered by the protective zones of the lightning poles, as defined by the rolling sphere method. Protection effectiveness shows a steady improvement from traditional to modern methods. GA provides a baseline protection coverage of 82%, while PSO and HGA-PSO achieve 85% and 88%, respectively. AI methods outperform these results, with ANNs achieving 91% and PINNs providing the highest protection score of 93%. The 11% difference between GA and PINN represents a significant increase in system reliability, potentially preventing costly lightning damage to sensitive PV components. The transformer models perform slightly below PINNs at 90%, while the RF maintains a remarkable protection score of 89%.

The *Grounding Error* measures the accuracy of the grounding system design predicted by the optimization algorithm. It is defined as the relative difference between the algorithm's predicted total grounding resistance ($R_{t\ predicted}$) and the target resistance ($R_{t\ target}$) calculated as necessary for safety in Level 2. Optimizing the grounding system is particularly challenging for traditional methods. GA exhibits an error rate of 12.3% in ground resistance calculations, while PSO reduces this to 9.7%. The combined HGA-PSO approach achieves an error rate of 7.1%, demonstrating the benefits of hybrid optimization strategies. AI methods show significant improvements in this critical parameter – ANN reduces errors to 5.9%, while PINN achieves an exceptional error rate of 3.2% through its physics-constrained architecture. This 74% error reduction compared to GA translates into more reliable fault current dissipation and improved system safety. The transformer models maintain their strong performance with an error of 4.1% and the RF with 6.7%.

Figure 3 provides a representation of the performance characteristics of the different ELPS optimization methods. The scatterplot divides the solution space into two distinct regions: metaheuristic methods (GA, PSO, HGA-PSO) cluster in the lower right quadrant and show slower convergence times and moderate accuracy, while AI-based approaches (ANN, PINN, Transformer, RF) dominate the upper left quadrant and achieve faster computations and superior protection scores. Notably, the position of PINN emerges as the most balanced solution, offering near-optimal performance in both dimensions. This visualization effectively demonstrates how hybrid approaches such as HGA-PSO act as transitional methods between the two clusters. At the same time, pure AI implementations push the Pareto frontier toward the ideal starting point of instantaneous and perfect accuracy.

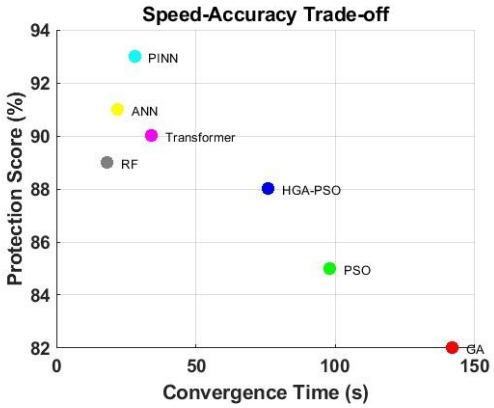

Fig. 3. Scatterplot of method performance

B. Comparative Analysis of AI

The performance benefits of AI methods are particularly evident when examining the trade-off between computational speed and accuracy. While meta-heuristic approaches require transaction speed for accuracy, AI models achieve both faster results and superior conservation metrics. PINNs emerge as the most balanced solution, combining physical fidelity with computational efficiency. Their ability to directly encode the fundamental equations in the network architecture ensures compliance with international standards while maintaining a practical design timeline.

Figure 4 shows the three-dimensional visualization critical for the performance trade-offs of different AI approaches. The Figure reveals that while RF offers the

lowest computational complexity at 0.7 MFLOPs, making it suitable for edge devices and rapid prototyping, it achieves only 89% protection with a relatively high 6.7% grounding error. At the other extreme, Transformer models demand 2.5 MFLOPs of computation but deliver only marginally better protection, about 90%, than simpler methods. The PINN method emerges as the most balanced solution, achieving the highest protection score with 93% and 1.8 MFLOPs computational requirements and a 3.2% grounding error. This performance of PINN is better than others because it can add fundamental physical equations directly into its architecture. So, it can solve solutions that comply with IEC standards based on Table I while maintaining computational efficiency. The ANN represents a middle ground, offering 91% protection at 1.2 MFLOPs, but with 5.9% grounding errors, it has a higher error than PINN. The results demonstrate that computational power (Transformers) does not guarantee optimal results, while PINN achieve better accuracy with reasonable computational demands. Therefore, for practical implementation, PINN should be the default choice. In comparison, RF remains applicable for quick assessments in resource-constrained environments.

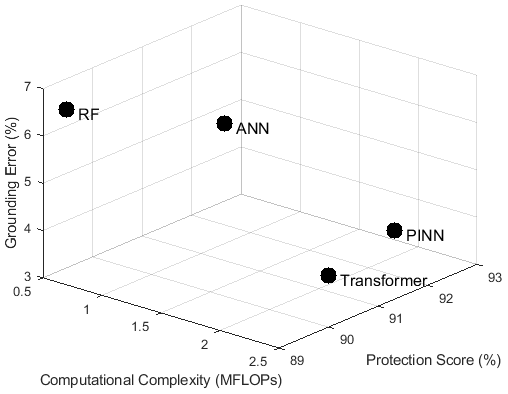

Fig. 4. 3D visualization of computational efficiency trade-off

Figure 5 illustrates that the radar chart provides a multidimensional comparison of four AI approaches for optimizing ELPS. The visualization demonstrates that PINN offer the most balanced performance profile, excelling particularly in grounding accuracy and protection coverage while maintaining reasonable computational efficiency. Its uniform shape on the sides indicates better performance than other models. In contrast, the RF model shows a sharply spiked profile, highlighting its exceptional computational speed and FLOP efficiency but significantly poorer performance in grounding system design. The Transformer model presents an interesting middle ground, with decent protection capabilities but higher computational demands, while ANN demonstrates competent all-around performance without any standout weaknesses. The radial format effectively communicates how each approach makes distinct trade-offs between physical fidelity and computational efficiency, with PINNs emerging as the most robust solution for comprehensive lightning protection system design in PV applications.

Figure 6 shows the performance of various models under the same data to estimate ELPS parameters. In this figure, the learning convergence of different AI approaches for ELPS design is presented. The logarithmic scale loss values show that PINN achieves the fastest convergence and the lowest final error. This demonstrates the effectiveness of incorporating physical constraints into the training process. While RF shows fast initial convergence, it reaches a steady state at a relatively high error level. The Transformer model shows slower initial progress but eventually outperforms the ANN in final accuracy, indicating that its attention mechanisms become increasingly effective with further training cycles. The ANN shows continuous improvement but cannot match the final accuracy of PINN, highlighting the value of physics-based regularization.

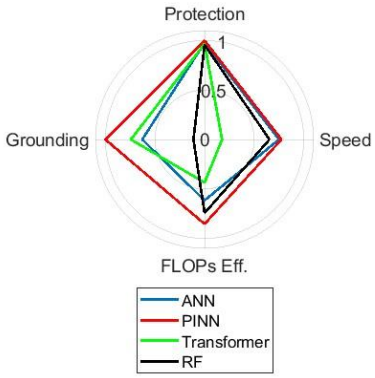

Fig. 5. Radar chart of AI model capabilities

The parameter sensitivity analysis in Figure 7 reveals fundamental differences in how each AI model prioritizes input variables for lightning protection system design. PINN demonstrates the most physically intuitive sensitivity profile, showing a strong dependence on soil resistivity with a value of 0.45. This contrasts sharply with RF, which overweight the PV area with a value of 0.35, while underweighting soil conditions with a value of 0.25, explaining its poorer grounding accuracy. The Transformer model shows balanced but somewhat diffuse sensitivity across parameters, while ANN's moderate sensitivity to protection level with a value of 0.35 reflects its data-driven approach. Notably, PINN's low sensitivity to thunder days, with a value of 0.08, suggests robust performance across varying weather conditions. Generally, the patterns show the sensitivity analysis of each model and the effect of each parameter in models. PINN's physics-aware architecture naturally emphasizes the most physically significant parameters, while data-driven methods like RF and ANN tend to overemphasize more readily measurable but less critical inputs. This is while the transformer model is less sensitive to data and can be considered a good advantage of this model. Figure 8 shows the failure probability comparison. Based on the results,

PINN has high reliability for lightning protection systems, with its 5.41% failure rate representing an improvement over Transformer and ANN models. The Transformer's intermediate 9.95% failure rate suggests its attention mechanisms provide some robustness benefits over conventional ANN. Furthermore, PINNs have a remarkable reduction compared to RF. These field validation results directly reflect each method's underlying architecture. In fact, PINN's physics-constrained design prevents unphysical solutions that could lead to protection failures, while RF's data-driven approach proves particularly vulnerable to edge cases not represented in training data.

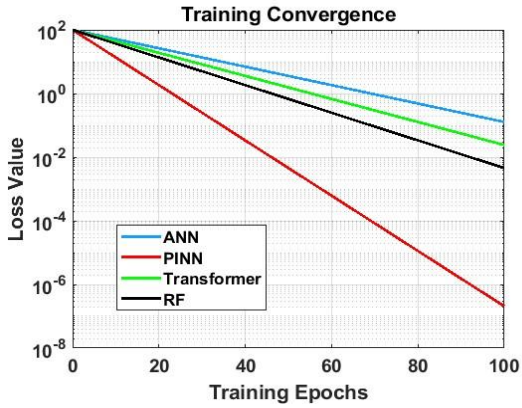

Fig. 6. Learning convergence curves results

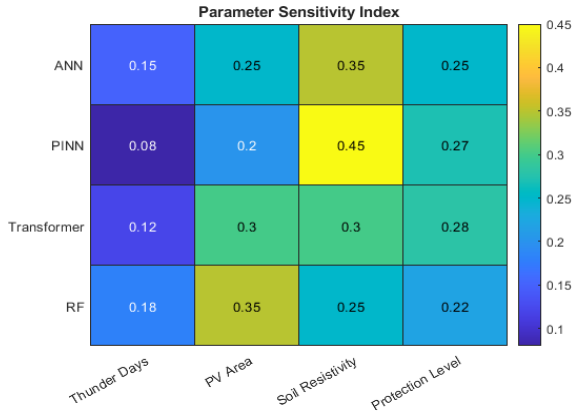

Fig. 7. Parameter sensitivity analysis of AI models

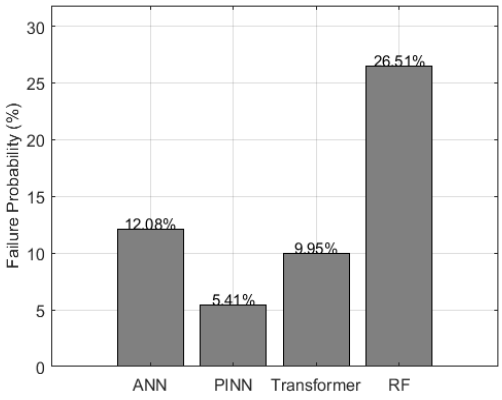

Fig. 8. Field failure probability comparison results

To strengthen the validation, new data are generated through simulation based on Table 2. A comparative study is conducted using the new data, and the results are analyzed and compared. The results are shown in Figures 9-11. Figure 9(a) shows the lightning protection coverage of each AI model. The PINN model achieves the highest protection score of 93%. The 2-4% difference between PINN and the other models indicates an improvement in system reliability in this AI model. ANN is the closest model in terms of protection capability with 91%, while Transformer and RF show lower protection effectiveness with 90% and 89%, respectively. Figure 9(b) shows the substantial differences in the accuracy of the ground system. In this case, PINN has a significant error rate of 3.2%. The Transformer model shows an acceptable performance with an error rate of 4.1%. In contrast, ANN and RF show higher error rates of 5.9% and 6.7%, respectively, indicating limitations in the design of the ground system. These results confirm the results of the comparative study conducted in the previous section.

Figure 10 presents both the protection score and grounding accuracy metrics. The results clearly demonstrate the dual superiority of PINN. The visual comparison emphasizes that the physics-based approach of PINN successfully bridges the gap between theoretical protection requirements and practical implementation constraints. These results also confirm previous results using new data. Figure 11 introduces a performance ratio metric (protection score divided by grounding fault) that quantifies the overall effectiveness of the system. PINN achieves the highest ratio of approximately 29.1, significantly outperforming other models. This metric effectively captures the essential balance between protection coverage and implementation accuracy, providing a single comprehensive measure of design quality.

Statistical analysis performed on several random samples conclusively shows that PINN achieves a strong and consistent performance advantage over other AI models. The results of this evaluation are shown in Table 4. The PINN model consistently achieved the highest average protection score and the lowest average ground fault across all 10 seeds. While models such as the standard ANN and Transformer showed greater sensitivity to initial conditions, the RF model also showed very low variance (±0.5% and ±0.4%) due to its ensemble nature, where the average is calculated over many decision trees. However, its average performance was lower than PINN. PINN consistently produced the highest protection score and the lowest ground fault with minimal deviation.

C. Recommended Implementation

Based on the comprehensive performance analysis of various optimization methods for ELPS in PV installations, the PINN model is offered as the most robust solution. It should perform as the primary design approach for most applications. PINN demonstrates good performance across

all critical metrics, achieving a 93% protection score with only 3.2% grounding error while maintaining reasonable computational efficiency. Its physics-constrained architecture provides unmatched reliability and has a lower failure rate compared to conventional ANN approaches and RF methods. This performance advantage stems from PINN's unique ability to use fundamental physical equations directly into the model. Using equations alongside training data significantly helps to obtain better results but may increase sensitivity and reduce performance speed, as shown in the results.

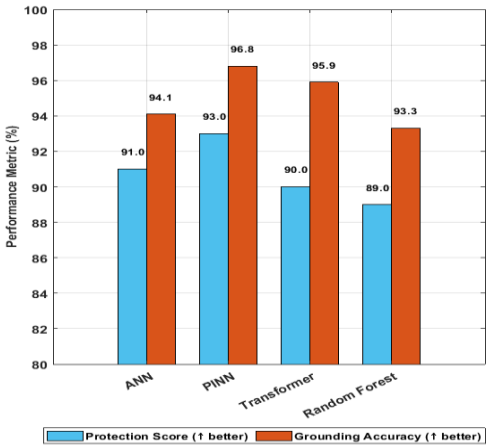

Fig. 9. Combined metrics of protection score and grounding accuracy

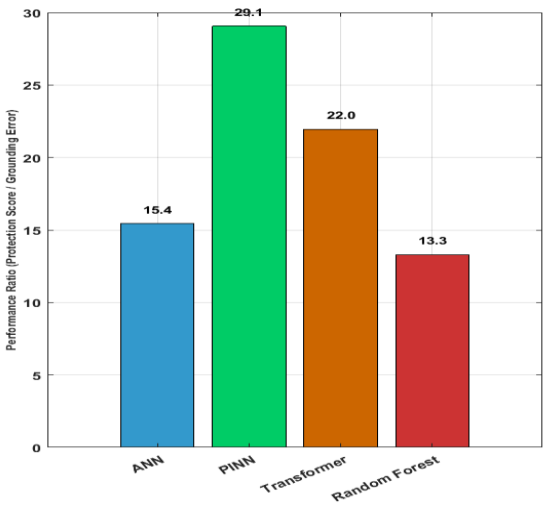

Fig. 10. Comprehensive analysis of protection system effectiveness

TABLE IV. Performance Metrics across 10 random seeds (Mean ± Standard Deviation)

Model	*Protection Score (%)*	*Grounding Error (%)*	*Convergence Time (s)*
PINN	92.7 ± 0.4	3.4 ± 0.3	29.1 ± 2.1
ANN	90.8 ± 0.7	6.1 ± 0.6	22.3 ± 1.8
Transformer	89.5 ± 1.1	4.3 ± 0.5	35.2 ± 3.0
RF	89.2 ± 0.5	6.9 ± 0.4	18.5 ± 1.2

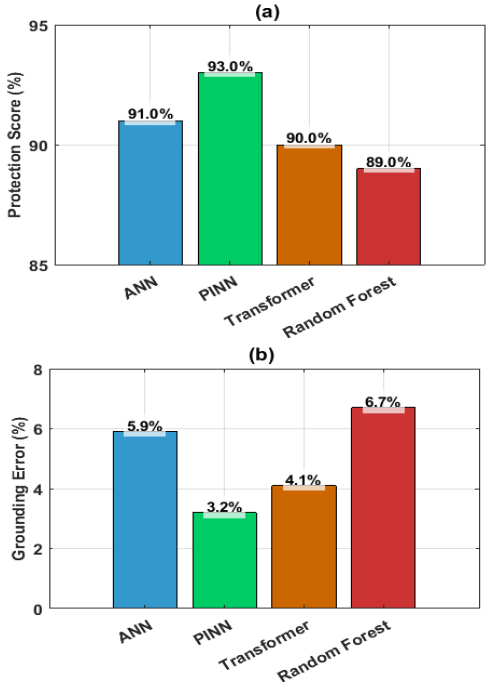

Fig. 11. Comparative validation of AI models for ELPS optimization based on new data. **(a)** Protection coverage score **(b)** Grounding system design error

Despite its demonstrated advantages, the proposed PINN approach has limitations. Its training phase is computationally more intensive than that of standard ANNs or RF due to the evaluation of physical equations. Furthermore, its performance is inherently tied to the accuracy of the underlying physical model; incorrect or oversimplified governing equations would lead to biased predictions. While PINNs reduce the demand for vast empirical datasets, they still require high-quality data to calibrate the physics to real-world conditions. Finally, the implementation complexity of PINNs is higher, requiring expertise in both machine learning and domain-specific physics. For large-scale PV installations, PINN should be implemented throughout the entire design workflow. It means from initial pole configuration using their multi-stage optimization framework to final grounding system design with their dual-path neural network approach. The RF method remains useful for rapid prototyping due to its computational efficiency, and Transformers offer value for complex spatial optimization in mega-scale farms. PINN provide the optimal balance of accuracy, reliability, and practical implementation requirements in PV protection. The method's consistent performance across varying contamination levels and weather conditions makes it particularly valuable for real-world deployment where environmental factors fluctuate significantly. However, the ANN is an option for smaller-scale PV. The ELPS design is not complex, and the pole numbers and their location are constraints.

V. Conclusions

This study presents a comparison of several AI-based optimization methods for designing lightning protection systems. Physics-based neural networks emerge as the most effective solution, outperforming traditional optimization methods and conventional machine learning approaches. Field validation results confirm the superior reliability of physics-based AI models, with a significantly lower failure rate compared to alternative approaches. For practical implementation, the findings indicate that large-scale photovoltaic installations benefit most from comprehensive PINN-based design workflows, while smaller systems may benefit from simpler ANN configurations. The behaviour of the RF model is also very similar to that of the ANN model. However, a large scatter is observed in the transformer model analysis. PINN demonstrates superior protection effectiveness with a 93% coverage score, significantly outperforming genetic algorithms at 82% and particle swarm optimization at 85%. In terms of grounding system accuracy, PINN achieves a remarkable 3.2% error rate, representing a 74% improvement over GA's 12.3% error rate. While random forest algorithms show the fastest convergence at 18 seconds, their 6.7% grounding error and 89% protection score prove less reliable than PINN's balanced performance at 28 seconds of computation time. The multi-level optimization framework successfully addresses critical interactions between air termination design and grounding parameters that single-stage methods often neglect. Field validation data confirms PINN's practical reliability with a 5.41% failure rate, nearly half that of transformer models at 9.95%.

Future research directions include the hybrid use of the proposed models at each of the optimization levels, which could yield even better results. Furthermore, adding more constraints, including optimal location, shadow size of the poles, and other limiting factors, can help design a more accurate and practical ELPS. Looking forward, this research opens several promising future directions. First, it can be investigated using hybrid modeling, where a PINN is used for the critical grounding system design, and a faster RF model is used for the air termination layout. Second, integrating additional practical constraints, such as dynamic shadow analysis, topological limitations, and detailed economic costing, into the optimization framework is a crucial next step. Finally, exploring transfer learning techniques for PINNs could drastically reduce their computational overhead for new, unseen site conditions, making this powerful approach more accessible.

REFERENCES

[1] P. Chiradeja and A. Ngaopitakkul, "Identify direct lightning strike location based on discrete wavelet transform for 115-kv transmission system," *IEEE Access,* vol. 10, pp. 80609-80622, 2022. doi: https://doi.org/10.1109/access.2022.3195497.

[2] I. Mousaviyan, S. G. Seifossadat, and M. Saniei, "A new and very fast fault detection and classification method based on traveling wave in transmission lines," *International Journal of Industrial Electronics Control and Optimization,* vol. 4, no. 4, pp. 377-385, 2021. doi: https://doi.org/10.22111/ieco.2021.38344.1348.

[3] Q. Wang, X. Liang, Y. Shen, S. Liu, Z. Zuo, and Y. Gao, "Lightning flashover characteristics of a full-scale AC 500 kV transmission tower with composite cross arms," *Engineering,* vol. 23, pp. 130-137, 2023.

[4] W. Qian *et al.*, "Mono-pole blocking accident analysis caused by inaccurate measurement of optical CT in±800 kV UHVDC transmission system under lightning strike," *Electric Power Systems Research,* vol. 239, p. 111212, 2025. doi: https://doi.org/10.1016/j.epsr.2024.111212.

[5] S. Mpanga, A. Zulu, M. Mwanza, and R. L. Holle, "Spatial and temporal variation of Zambia lightning for designing lightning protection of infrastructure," *Electric Power Systems Research,* vol. 229, p. 110188, 2024. doi: https://doi.org/10.1016/j.epsr.2024.110188.

[6] B. RAHEEM, E. Ogbuju, and F. Oladipo, "Development of a Lightning Prediction Model Using Machine Learning Algorithm: Survey," *Journal of Applied Artificial Intelligence,* vol. 4, no. 1, pp. 45–56-45–56, 2023. doi: https://doi.org/10.48185/jaai.v4i1.727.

[7] I. M. Y. Negara, D. Fahmi, D. A. Asfani, I. S. Hernanda, R. B. Pratama, and A. B. Ksatria, "Investigation and improvement of standard external lightning protection system: Industrial case study," *Energies,* vol. 14, no. 14, p. 4118, 2021. doi: https://doi.org/10.3390/en14144118.

[8] A. Ozdemir and S. Ilhan, "Experimental performance analysis of conventional and non-conventional lightning protection systems–preliminary results," *Electric Power Systems Research,* vol. 216, p. 109080, 2023. https://doi.org/10.12973/ijem.6.2.259.

[9] K. Sobolewski and E. Sobieska, "Analysis of the effectiveness of lightning and surge protection in a large solar farm," *Archives of Electrical Engineering,* vol. 71, no. 2, 2022 doi: https://doi.org/10.24425/aee.2022.140726.

[10] M. Gonçalves, E. da Costa, A. Andrade, V. Brito, G. Lira, and G. Xavier, "Grounding system models for electric current impulse," *Electric Power Systems Research,* vol. 177, p. 105981, 2019. doi: https://doi.org/10.1016/j.epsr.2019.105981.

[11] A. K. Mishra, N. Nagaoka, and A. Ametani, "A genetic algorithm approach for modeling a grounding electrode," *IEEJ Transactions on Power and Energy,* vol. 125, no. 8, pp. 816-821, 2005. doi: https://doi.org/10.1541/ieejpes.125.816.

[12] S. He *et al.*, "Intelligent prediction of 110kV insulator lightning flashover criteria based on random forest," *Electric Power Systems Research,* vol. 232, p. 110423, 2024. doi: https://doi.org/10.1016/j.epsr.2024.110423.

[13] H. R. Sezavar and S. Hasanzadeh, "Artificial Intelligence for Assessing Composite Insulator Pollution Level: A Study on Partial Discharge Characteristics," *International Journal of Industrial Electronics Control and Optimization,* 2025. doi: https://doi.org/10.22111/ieco.2025.51554.1680

[14] J. M. Martínez, E. M. N. Angarita, J. R. N. Alvarez, M. H. Crespo, and P. J. F. Pertuz, "Lightning rod system: mathematical analysis using the rolling sphere method," *International Journal of Power Electronics and Drive*

Systems (IJPEDS), vol. 13, no. 1, pp. 2829-2838, 2022. doi: https://doi.org/10.11591/ijpeds.v13.i1.pp237-246.

[15] M. Alves *et al.*, "An automated technique and decision support system for lightning early warning," *International Journal of Environmental Science and Technology,* vol. 22, no. 4, pp. 2289-2304, 2025 .doi: https://doi.org/10.1007/s13762-024-05693-7.

[16] R. Bao, Y. Zhang, B. J. Ma, Z. Zhang, and Z. He, "An artificial neural network for lightning prediction based on atmospheric electric field observations," *Remote Sensing,* vol. 14, no. 17, p. 4131, 2022. doi: https://doi.org/10.3390/rs14174131.

[17] M. Bhosale, P. B. Karandikar, V. Karkaria, and N. R. hKulkarni, "A novel approach for grounding resistance estimation," *Indones. J. Electr. Eng. Comput. Sci,* vol. 27, p. 583, 2022. doi: https://doi.org/10.11591/ijeecs.v27.i2.pp583-591.

[18] K. Mehranzamir, Z. Abdul-Malek, H. N. Afrouzi, S. V. Mashak, C.-l. Wooi, and R. Zarei, "Artificial neural network application in an implemented lightning locating system," *Journal of Atmospheric and Solar-Terrestrial Physics,* vol. 210,p.105437,2020.https://doi.org/10.1016/j.jastp.2020.105437.

[19] C. Wang, X. Zhang, H. Yang, J. Guo, J. Xu, and Z. Sun, "Application research of convolutional neural network and its optimization in lightning electric field waveform recognition," *Scientific Reports,* vol. 15, no. 1, p. 1883, 2025. doi: https://doi.org/10.1038/s41598-025-85473-6

[20] R. Rohana, S. Hardi, N. Nasaruddin, Y. Away, and A. Novandri, "Multi-Stage ANN Model for Optimizing the Configuration of External Lightning Protection and Grounding Systems," *Energies,* vol. 17, no. 18, p. 4673, 2024. https://doi.org/10.3390/en17184673.

[21] S. Kumar, G. Singh, and N. Ahamad, "Performance of 5 Years of ESE Lightning Protection System," in *Clean and Renewable Energy Production*, 2024, pp. 247-265. https://doi.org/10.1002/9781394174805.ch10

[22] M. Parhamfar, R. Naderi, and I. Sadeghkhani, "Risk assessment, lightning protection, and earthing system design for photovoltaic power plants: A case study of utility-scale solar farm in Iran," *Solar Energy Advances,* vol. 5, p. 100098, 2025/01/01/ 2025. https://doi.org/10.1016/j.seja.2025.100098.

[23] J.-W. Tang, V. Cooray, C.-L. Wooi, M. Z. A. Ab Kadir, W.-S. Tan, and H. N. Afrouzi, "Optimization of Lightning Protection System Using Multi-Objective Optimization Techniques," in *ICLP 2024; 37th International Conference on Lightning Protection*, 2024, pp. 620-625: VDE. doi : https://doi.org/10.1109/ICPEI61831.2024.10748622

[24] M. Nassereddine, H. Ahmed, E. Barbulescu, J. Rizk, A. Hellany, and M. Nagrial, "Direct Lightning Protection for PV Systems; A Novel Approach to Eliminate Shading Effects," in *2024 International Conference on Electrical, Computer and Energy Technologies (ICECET*, 2024, pp. 1-6: IEEE. https://doi.org/10.1109/icecet61485.2024.10698474.

[25] N. Rodrueang, S. Woothipatanapan, N. Charlangsut, P. Ngamprasert, N. Ruangsap, and N. Rugthaicharoencheep, "Risk Assessment of the Lightning Protection System for Hybrid Solar Power Generation Rooftop System on the Factory Using the FMECA Technique," in *2024 International Conference on Power, Energy and Innovations (ICPEI)*, 2024, pp. 167-172: IEEE. https://doi.org/10.1109/ICPEI61831.2024.10748622

[26] M. Nassereddine, "A novel lightning mast layout to eliminate shading effect on PV panels," *Electric Power Systems Research,* vol. 236, p. 110972, 2024. doi: https://doi.org/10.1016/j.epsr.2024.110972.

[27] Negara, I. Made Yulistya, et al. "Investigation and improvement of standard external lightning protection system: Industrial case study." Energies 14.14 (2021): 4118. doi: https://doi.org/10.3390/en14144118.

[28] V. P. Androvitsaneas, I. F. Gonos, and I. A. Stathopulos, "Research and applications of ground enhancing compounds in grounding systems," *IET Generation, Transmission & Distribution,* vol. 11, no. 13, pp. 3195-3201, 2017. doi: https://doi.org/10.1049/iet-gtd.2017.0233.

[29] M. Wahba, M. Abdel-Salam, M. Nayel, and H. A. Ziedan, "Experimental characterization of contact resistance of desert soil with waste-enhancement materials in grounding systems," *Results in Engineering,* vol. 23, p. 102707, 2024. doi: https://doi.org/10.1016/j.rineng.2024.102707.

[30] O. Kherif, S. Robson, H. Griffiths, N. Harid, D. Thorpe, and A. Haddad, "On the high frequency performance of vertical ground electrodes and LRM application," *IEEE Transactions on Electromagnetic Compatibility,* 2024. doi: https://doi.org/10.1109/temc.2024.3435788.

[31] L. Neamț, O. Chiver, C. Barz, C. Costea, and Z. Erdei, "Considerations about power system grounding for different soil structure," in *2014 International Conference and Exposition on Electrical and Power Engineering (EPE)*, 2014, pp. 1034-1038: IEEE. doi: https://doi.org/10.1109/icepe.2014.6970066.

[32] B. Kermani and R. Shariatinasab, "Protection of Photovoltaic Systems Against Direct Lightning Strokes," *IEEE Transactions on Power Delivery,* 2024. https://doi.org/10.1109/tpwrd.2024.3494053.

[33] R. De Franco *et al.*, "Monitoring the saltwater intrusion by time lapse electrical resistivity tomography: The Chioggia test site (Venice Lagoon, Italy)," *Journal of Applied Geophysics,* vol. 69, no. 3-4, pp. 117-130, 2009. doi: https://doi.org/10.1016/j.jappgeo.2009.08.004.

[34] P. against Lightning-Part, "3: Physical damage to structures and life hazard," *International Electro-technical Commission. IEC,* pp. 62305-3, 2010. doi: https://doi.org/10.4324/9780203805305.

[35] P. K. Samaras *et al.*, "Evaluation of the electric stress on an Insulating down-conductor caused by lightning strikes through ATP-EMTP simulations," *IEEE Transactions on Industry Applications,* 2024. doi: https://doi.org/10.1109/tia.2024.3429472.

[36] A. G. Martins-Britto, C. M. Moraes, and F. V. Lopes, "Transient electromagnetic interferences between a power line and a pipeline due to a lightning discharge: An EMTP-based approach," *Electric Power Systems Research,* vol. 197, p. 107321, 2021. doi: https://doi.org/10.1016/j.epsr.2021.107321.

[37] B. Huang and J. Wang, "Applications of physics-informed neural networks in power systems-a review," *IEEE Transactions on Power Systems,* vol. 38, no. 1, pp. 572-588, 2022. doi: https://doi.org/ 10.1109/TPWRS.2022.3162473

[38] R. Labib, "Utilizing physics-informed neural networks to advance daylighting simulations in buildings," *Journal of Building Engineering,* vol. 100, p. 111726, 2025. doi: https://doi.org/10.1016/j.jobe.2024.111726.

[39] L. Zhang, Z. Zhang, S. Fang and A. S. Bretas, "An Optimization Model for Distribution Networks Lightning Protection System Design: a Reliability Indexes and Cost-based Solution," 2020 IEEE Power & Energy Society

General Meeting (PESGM), Montreal, QC, Canada, 2020, pp. 1-5, doi: 10.1109/PESGM41954.2020.9281988.

[40] N. Fahimi, H. Sezavar, and A. Shayegani-Akmal, "Flashover prediction of polymer insulators based on dynamic modeling of pollution layer resistance using ANN," *IEEE Transactions on Dielectrics and Electrical Insulation,* vol. 30, no. 1, pp. 122-130, 2022. doi: https://doi.org/10.1109/tdei.2022.3207452.

[41] N. Fahimi, H. R. Sezavar, and A. A. S. Akmal, "Dynamic modeling of flashover of polymer insulators under polluted conditions based on HGA-PSO algorithm," *Electric Power Systems Research,* vol. 205, p. 107728, 2022. doi: https://doi.org/10.1016/j.epsr.2021.107728.

[42] M. R. Masoudi, M. Haghighi, and H. R. Sezavar, "Optimization of Energy Hub Performance Using the Improved Particle Swarm Optimization (IPSO) Algorithm for Integrated Energy Systems," in *2025 12th Iranian Conference on Renewable Energies and Distributed Generation (ICREDG)*, 2025, pp. 1-6: IEEE. doi: https://doi.org/10.1109/ICREDG66184.2025.10966138.

Hamid Reza Sezavar was born in Qom, Iran, in 1991. He received a B.Sc. degree from the Sharif University of Technology, Tehran, Iran, in 2013 and a M.Sc. in electrical engineering from the University of Tehran, Tehran, Iran, in 2015. He then received his PhD in High Voltage from the University of Tehran, Tehran, Iran, in 2022. He is currently working toward an assistant professor position at Qom University of Technology. His principal research interests are High voltage engineering, outdoor insulators, and Electrical discharge, Lightning, and AI algorithms.

Appendix A

AI	Artificial Intelligence
ANN	Artificial Neural Network
ELPS	External Lightning Protection System
GA	Genetic Algorithm
HGA-PSO	Hybrid Genetic Algorithm - Particle Swarm Optimization
IEC	International Electrotechnical Commission
PINN	Physics-Informed Neural Network
PSO	Particle Swarm Optimization
PV	Photovoltaic
RF	Random Forest

Appendix B

1. Neural Network Architectures & Hyperparameters

All neural network models (ANN, PINN, Transformer, and RF) are implemented using TensorFlow v2.8 and Keras. The models for each of the three optimization levels shared similar base architectures but were tailored to their specific input-output dimensions.

- ANN Architecture:
  - Structure: A feedforward network with 3 hidden layers.
  - Layer Sizes: Input Layer → (128 neurons) → (64 neurons) → (32 neurons) → Output Layer.
  - Activation Functions: ReLU for all hidden layers. Linear activation for the output layer (suitable for regression).
  - Initialization: He Normal initialization.
  - Regularization: L2 regularization (λ = 0.001) was applied to the kernel weights of each layer to prevent overfitting.
- PINN Architecture:
  - Structure: The PINN shared the same base architecture as the ANN (128-64-32) to ensure a fair comparison.
  - Physics-Informed Component: The physics loss was calculated based on the governing equations (Eqs. 4, 5, 6 for grounding; Eqs. 1, 2, 3 for air termination) and added to the standard mean squared error (MSE) data loss.
  - Loss Function: Total_Loss = MSE (Data) + λ * MSE (Physics), where the physics constant λ was set to 0.5 after a sensitivity analysis. This enforced that the network's predictions adhered to physical laws.
- Transformer Architecture:
  - Structure: 2 Transformer encoder blocks.
  - Key Parameters: Embedding dimension = 64, Number of heads = 4, Feedforward dimension = 128.
  - Input Processing: The tabular data was first projected into a higher-dimensional space using a dense layer. A learnable positional encoding was added, as the order of the input parameters (e.g., Td, Apv, ρ) is not sequential.
  - Output: The [CLS] token output from the final encoder block was passed through a 3-layer MLP (64 → 32 → output) to generate the prediction.
- Random Forest (RF):
  - Number of Trees: 100 estimators.
  - Other Parameters: max_depth = None (nodes expanded until pure), min_samples_split = 2, min_samples_leaf = 1. These parameters were chosen to allow the model to fully fit

the training data without excessive constraint.

2. Training Parameters & Hyperparameter Tuning

- Common Training Parameters:
    - Optimizer: Adam.
    - Learning Rate: A starting learning rate of 0.001 was used for all models, with a reduction by a factor of 0.5 if the validation loss plateaued for 10 epochs.
    - Batch Size: 32.
    - Train/Validation/Test Split: 70%/15%/15%. The split was performed randomly but consistently across all models to ensure a fair comparison.
    - Epochs: Training was stopped early if the validation loss did not improve for 25 consecutive epochs (Early Stopping callback), preventing overfitting. The maximum number of epochs was set to 500.
- Hyperparameter Tuning Process:
    - A Bayesian Optimization process was conducted using the Hyperopt library for the neural networks (ANN, PINN).
    - Search Space:
        - Number of hidden layers: [2, 3, 4]
        - Number of units per layer: [32, 64, 128, 256]
        - Learning Rate: Log-uniform distribution between 1e-4 and 1e-2
        - L2 Regularization (λ): [1e-4, 1e-3, 1e-2]
    - The objective was to minimize the Mean Absolute Error (MAE) on the validation set.
    - The final architectures and parameters reported above represent the best configuration found after 50 trials for each model type.